GENERATION OF CHANNEL MEANDERING

Dr. N.L. Dongre, IPS, Ph.D., DLitt**

Narmada River meandering at Bhedaghat, Jabalpur which flow through a channel with modifiable boundaries and carved plan form sets up internal flow instabilities.

Abstract: ***Traced by fluid flows, Meander patterns are a ubiquitous feature of physical landscapes on Earth, Mars, the volcanic floodplains of the Moon and Venus and other planetary bodies. Discussed especially as a result of migration processes in meandering rivers, Meandering is also denotes in channel types that express little or no indication of meandering. Meandering is seldom described as "inherited" from a pre-existing structure, which still does not explain where the inherited Meandering appeared from. For a phenomenon so universal as Meandering, existing models of channelized flows do not describe the occurrence of Meandering in***

****Dr. N.L. Dongre**
C-14 Jaypee Nagar Rewa 486450
Email: - nl.dongre@jalindia.co.in dongrenl@gmail.com
Mobile No. 7869918077, 09425152076

the full variety of settings in which it manifests, or how Meandering may originate. Here it is presented that the theory for Meander flow patterns in landscapes. Using observations from nature and a numerical model of flow routing, proposed that flow resistance (representing landscape roughness attributable to topography or vegetation density) relative to surface slope exerts a fundamental control on channel Meandering that is effectively independent of internal flow dynamics. Resistance-dominated surfaces produce channels with higher Meandering than those of slope-dominated surfaces because increased resistance impedes downslope flow. Not limited to rivers, the hypothesis explored pertains to Meandering as a geo-morphic pattern. The explanation proposed is inclusive enough to account for a wide variety of Meander channel types in nature, and can serve as an analytical tool for determining the Meandering a landscape might support.

Keywords:- Geopatterns , Landscape controls ,Threadlike flows ,Meandering.

Meander, threadlike flows are omnipresent features of landscapes on Earth and other planetary bodies (Fig. 1). Meandering is specifically discussed as a result of channel migration processes in meandering rivers (1-9), where flow through a channel with modifiable boundaries and a curved plan form sets up internal flow instabilities that drive spatial patterns of bank erosion and accretion, which change plan form curvature. The physical mechanisms by which a nearly straight channel evolves into a freely meandering planform have been studied intensively and with great success. Strath terraces and meander bend cutoffs are evidence that even bedrock river channels can migrate, adjusting their Meandering over time (10, 11). Despite their prominence, rivers with migrating meanders are a subset of the Meander channel types that exist: lunar and Venusian rilles (12, 13) are Meander, static patterns in lava channels; drainage channels in tidal mudflats that show little or no morphologic evidence of migration behavior can be characterized as quasi-static Meander patterns (14-16). Meandering in some channels is described has having been "inherited" from a preexisting morphology (10, 14), but the nature of the antecedence tends to be unspecific or unexplained.

It is true that every Meander, threadlike flows engage from effectively straight original planforms, then planform meandering as a geomorphic system is not inherently contingent upon a capacity to migrate. It is put up that a theory for meandering in threadlike flows (which it is referred here to as channel meandering for simplicity). It is used that an exploratory flow-routing model to show that changing the variance of flow resistance in the landscape (e.g., representative of local topographic roughness or vegetation density) relative to mean landscape slope produces a range of Meander patterns with natural analogs. A surprising relationship between Meandering and floodplain roughness relative to valley slope for 20 rivers from around the globe yields an independent test of the theory. It is suggested that this ratio of flow-resistance variance (R) to slope (S) exerts a primary landscape control on path Meandering (Ω) both in static and dynamic patterns of flow.

Numerical Model

The model is a cellular topography in which flow takes a path of less resistance across a planar domain of slope S superimposed with random values between 0 and R (Fig. 2). Because slope imposes a simple flow direction, the model follows the rules of a directed Brownian walk. Similar minimum-resistance simulations have been applied previously to mathematical structures and self-organization in natural fluvial systems and networks (17, 18), and have long-standing precedence in percolation theory (19) and theoretical material physics (20).

The domain landscape is the plane

$$z = -S \cdot x + (S.L), \tag{1}$$

where z is domain elevation and L is the length of the domain in the x direction (the plane extends in the y direction). Subtracting random topographic perturbations with values 0-R adjusts the elevation by

$$z_{ij} = -S \cdot x_{ij} + (S \cdot L) - r_{ij,} \tag{2}$$

where $r_{ij,}$ is the perturbation at a given cell ($i\ j$). The results presented here are for a square domain of L = 100 with non-periodic boundaries. (In terms of fluvial valleys, it is assuming that the domain length and down valley length are the same.) It varies R and S at increments equal to 0.001 over the interval 0.001-0.1 to generate domains with R/S ratios between 0.01 and 100.

The flow path follows the local gradient between nearby cells, occupying whichever of its eight neighbors has the lowest value. Length of the flow path (P) relative to the length of the domain (L) yields the path Meandering ($\Omega = P/L$). When the random perturbations are much smaller than the landscape gradient ($R << S$), the flow path always occupies one of three right-hand neighbor cells because their elevations are locally always the lowest. Conversely, when the magnitude of R overwhelms down-slope differences ($R >> S$), the flow becomes effectively undirected. Rather than always traveling downslope, the flow path is as or more likely to occupy a lateral or rear-flanking neighbor and trace a more excursive (Meander) route.

Three numerical artifacts come from this model design. First, when $R >> S$, the lowest-neighbor rule can result in an arbitrary configuration of neighbors that traps the flow path in an infinite loop. To override this arbitrary trapping, flow-occupied cells are temporarily assigned the unperturbed cell elevation (Eq. 1),

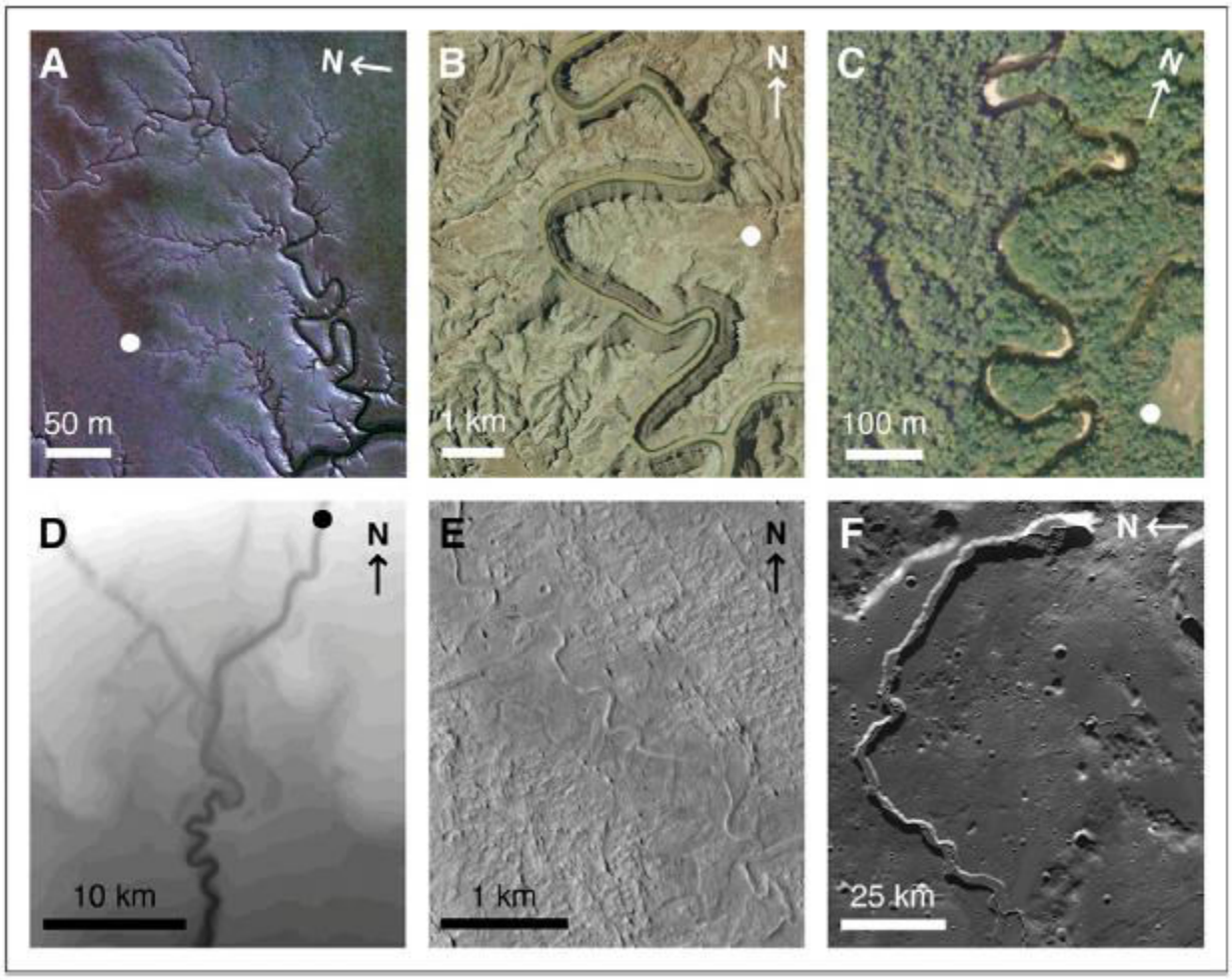

Figure. 1. Meander channels in *(A)* intertidal mudflat channels near Seoul, South Korea; *(B)* river channels in bedrock southwest of Moab, Utah; *(C)* a migrating reach of the Ellis River in Maine; *(D)* digital elevation model of submarine channels offshore of Rio Doce, Brazil; *(E)* relict fluvial channel patterns in the Aeolis Planum on Mars; and *(F)* a lunar volcanic rille in the Vallis Schroteri.

constituting a local high that discourages but does not prevent the path from recrossing itself. Recrossed cells are not double counted in the path length. The second artifact derives from the discretized cellular domain. A move to a cardinal neighbor adds unit length equal to 1 to the flow path; a move to an ordinal (diagonal) neighbor adds unit length equal to $\sqrt{2}$. Because flow moves to the lowest-elevation neighbor even when differences between downslope neighbors are infinitesimal, flow paths with $\Omega = 1$ only occur in the absence of topographic perturbations ($R = 0$). Therefore, when $0 < R << S$, the discretized domain always produces meanderings $1 < \Omega < 1.4$ (occupation only of downslope, ordinal neighbors produces $\Omega = 1.4$). At the other extreme, when $R >> S$, path Meandering loses physical significance and becomes an undirected Brownian walk. Mathematically, Meandering can be infinitely large, but highly Meander natural channels, such as in rivers with freely migrating meanders, express $\Omega \sim 3$ (2, 21). It is addressed that this Brownian artifact of exaggerated meandering as follows. Once a flow path is complete, it is assigned that the flow-occupied cells elevations according to

$$z_{ij} = -S \cdot x_{ij} + (S \cdot L) - R, \tag{3}$$

which ensures that the flow path contains the lowest local elevations in the domain (Fig. 2). It is rerun the flow-path simulation for 10 iterations, ammending the domain each time, so that the path adjusts to a minimum length for the specified conditions (Fig. 3). Flow paths through slope-dominated domains *(R/S* << 1) lock into their minimum Meandering on the first iteration; highly excursive planforms through resistance-dominated domains *(R/S* >> 1) find less Meander flow paths after a few iterations (Fig. 3). This rule is functionally analogous to meander cutoff in channels with migrating bends, but is not explicitly mechanistic.

Results

Results from over 30,000 flow-routing simulations (Fig. 4) indicate how path Meandering (Ω) responds to changes in resistance variance relative to slope *(R/S).* When slope increases the resistance term *(R/S* < 1), paths find the lowest meanderings allowed by the model's discretized domain (mean Meandering for all *R/S* < 1 is approximately Ω~ 1.28 ± 0.04). In the vicinity of *R/S* ~ 1, Ω begins to increase; with increasing values of *R/S* > 1, the variance of Ω scales with mean Ω (Fig. 5). Fourier analysis of flow paths exhibits no preferred wavelength in the modeled planforms (Fig. 5B). These characteristics explain the model's underlying Brownian mechanics, with the strength of resistance (*R*) relative to slope (*S*) driving the transition between directed and undirected random walks.

It is interesting to note that the upper range of planform meanderings generated with and without our iterated, minimum-path procedure are consistent with results of other numerical planform models whose channel patterns, with and without meander cutoffs, derive from parameterization of in-channel flow (3, 4, 22). However, unlike in other models, our flow paths are static once formed. It does not route flow around contortions in curvature (8, 9) or explicitly treat means by which channel geometries evolve (17, 23). The simulations may be interpreted as initial flow paths, perhaps most readily applicable to fixed flow planforms like volcanic rilles. Initial planforms can also arise anywhere initially unchannelized flow interacts with a mobile bed, incising a Meander planform as a function of valley slope and flow resistance. Where planform patterns may be described as quasi-static, an original Meandering may persist as a kind of legacy effect in planform evolution (10, 14, 24). In the special context of freely migrating channels, these initial planforms may be transitory patterns that hydraulic properties of in-channel flow subsequently rework.

Intertidal Channels in mudflats create an explanation. Meander drainage channels can incise fast into a mudflat and persist for many decades with few discernible change (14-16). Letting the generalizing assumption that intertidal mudflats participate broadly identical material properties (e.g., fine-grained, cohesive sediment), then to the first approximation it can compare channel paths in different mudflats on the basis of slope. For an arbitrary, low fixed resistance *R,* the model generates channel planforms on

steep *(R/S* < 1; Fig. 6 *A* and *B*) and gentle slopes (*R/S* > 1; Fig. 6 *C* and *D*) that resemble channels in comparable mudflats, respectively. Likewise, simulations in which channel Meandering adjusts across a

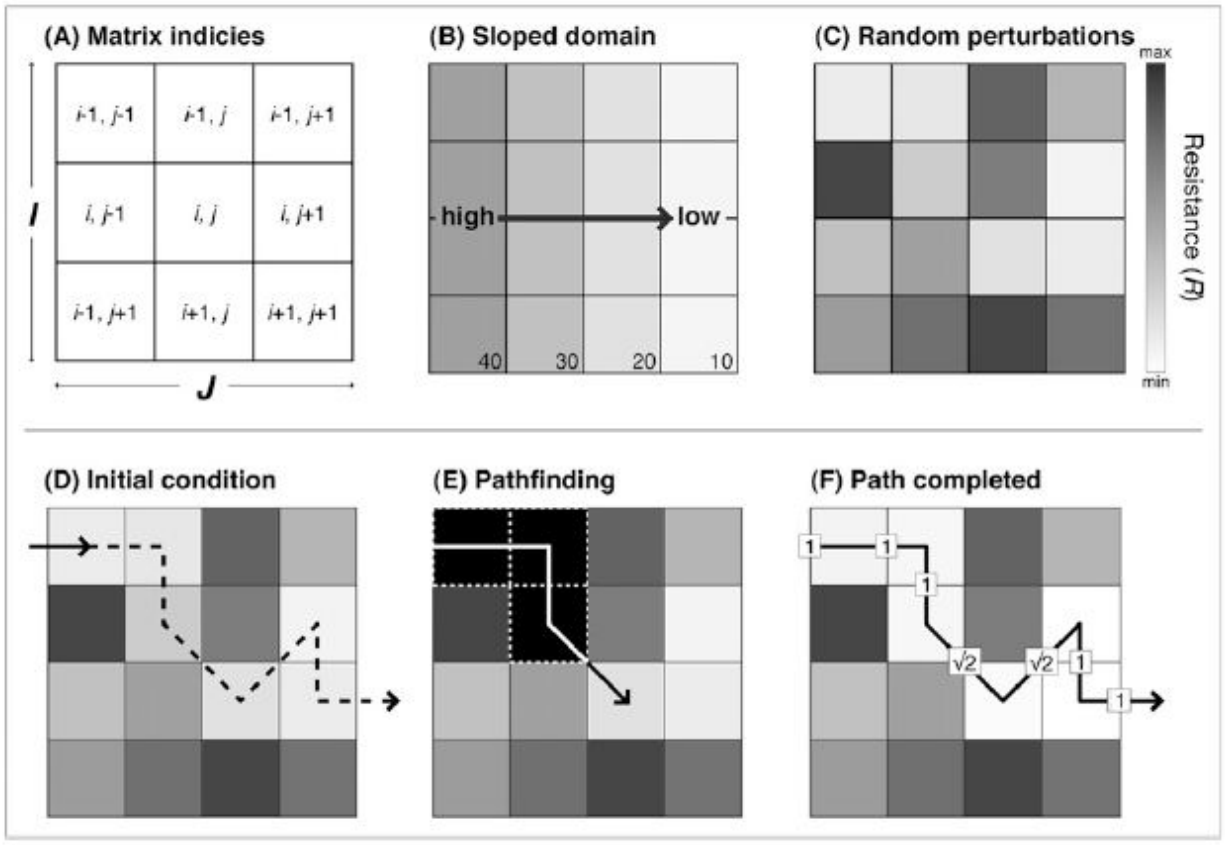

Figure. 2. Schematic of operations in this numerical flow-routing model. (*A)* Matrix indices relative to the center grid cell. (*B*) The parameter *S* determines the slope of the domain, from which (*C*) random values *0-R* are subtracted. (*D*) From a given cell, the flow path moves to occupy whichever of its nearest neighbors has the lowest value. (*E*) As the flow path is developing, values of cells that the flow has occupied are temporarily reset to the unperturbed elevation at that cell, as in B. This value constitutes a local maximum that discourages the flow path from getting arbitrarily trapped by a local minimum, but does not necessarily prevent the path from recrossing itself, particularly when *R* >> *S.(F)* Once completed, cells occupied by the flow path are reset equal to the domain elevation given by *B*, minus the maximum perturbation *R*. Meandering is the total length of the flow path (arrows show the respective lengths of straight and diagonal steps) divided by the length dimension of the domain. The flow path in the schematic above, excluding the steps into and out of the grid, has Meandering Ω = 5.82 ÷4 = 1.5.

break in slope are substantiated by examples in the field (25) (Fig. 6 *E* and *F*). For example, using a mean slope of *S* ~ 0.005 from *A* to *A′* (25) and a Meandering of *Ω* ~ 1.9 measured from *A* to *A′* in Fig. 6*E*, it can be applied that the relationship of Ω to *R/S* in Fig.4 to find an approximate value of *R* = 0.05. Entering these values for *R* and *S* into the model delivers a channel with Meandering *Ω* = 2.0 between *A* and *A′* (Fig. 6F). Relative to the steeper mean slope of *S* ~ 0.04 between B and B' (25), the same resistance *R* = 0.05 predicts a Meandering of Ω ~ 1.3. From Fig. 6 E, Meandering between B and B' is approximately *Ω* ~ 1.1; the corresponding modeled Meandering in Fig. 6 F is *Ω* = 1.2.

Counting the relationship in Fig. 4 to back out a value for *R* based on measurements of *S* and Ω produces an intriguing comparison but does not constitute a free test of the data. For that, it is offered that the following derivation, the relationship *R/S* is, essentially, a surrogate form of the Froude number,

which similarly can be expressed in terms of slope and a parameter for flow resistance. The standard formulation of the Froude number (F) for open-channel flow is

$$F = \frac{v}{\sqrt{gh}}, \tag{4}$$

where v is cross-sectional mean flow velocity, g is acceleration due to gravity (g = 9.81 m s^{-1}), and h is uniform flow depth. It can be expressed v according to the Gauckler-Manning formula,

$$v = \frac{1}{n} h^{2/3} S^{1/2}, \tag{5}$$

where S is slope and n is the empirically derived Gauckler-Manning coefficient, or Manning's n (s m$^{-1/3}$). Substituting Eq. 5 into Eq. 4 yields an expression of the Froude number based on characteristics of the floodplain, rather than the channel:

$$F = \frac{S^{1/2} h^{1/6}}{g^{1/2} n}. \tag{6}$$

It is estimated the floodplain Froude numbers for 20 meandering rivers around the world, assuming steady, uniform flow conditions and the same depth of inundation across each floodplain (h = 1 m; $h^{1/6}$ makes F relatively insensitive to this simplification). Manning's n has been calibrated for a variety of floodplain settings. Because F is sensitive to chosen values of n, and limit n to three possible values based on three observable conditions of predominant floodplain vegetation (26): grasses or row crops (n = 0.05); brush and some trees (n = 0.10); or trees with dense understory (n = 0.15). Values for valley slope (S) were obtained from the literature. The resulting data (Fig.7 *A)* suggest that valley slope relative to resistance—the prevailing floodplain conditions S and n—explains ~88% of the variability in planform Meandering. These data fall neatly among the ensemble minimum meanderings generated by the model (Fig. 7 B) when the model data are inverted (expressed in terms of S/R) to match the Froude number convention. Artificially high Meanderingin the model when $R/S >> 1$ (or, equivalently, when $S/R << 1$) skews the mean Meandering toward higher values, even with the path-iteration rule; it is therefore expect better observational agreement with modeled Meandering minima than with the means, especially given the rarity with which natural freely migrating meandering rivers exhibit $\Omega > 3$.

The abstraction of in-channel dynamics does not refute or discount the value of secondary flow mechanics. The remnant of the initial planform may be statistical, retained more in the morphometry of the related planform than expresses in its morphology. Where meander-migration theory forcast a preferred meander wavelength for a channel, the random-walk mechanism in this model produces a broad spectrum of wavelengths resembling brown noise (Fig. 5 *B*). This is consistent with empirical observations that not all rivers express a dominant wavelength (27, 28). The model delivers the initial Meandering of a new channel; that Meandering may change with modifications to the channel planform driven by dynamics of in-channel flow. If resistance and slope set the initial planform condition that subsequent meander-migration dynamics amend, then the broad-spectrum properties of the initial planform mean that there will always be perturbations present with the wavelength (or wavelengths) that meander migration will tend to amplify. Even without incorporating the dynamics of in-channel flow that enable natural, single-thread fluvial systems to develop characteristic meander wavelengths, our model offers an explanation for the important implications of Fig. 7 : that F is an important control on the long-term Meandering that freely meandering rivers attain. In this setting, the flow paths in our model are more directly analogous to avulsions or overbank flows, extra channel departures for which the effects of variable flow resistance might supersede in-channel dependencies, at least temporarily. The correlation between Ω and F in Fig. 7 reflects in part the role of overbank flows in modifying planform Meandering. As in-channel dynamics lengthen the channel, incising overbank flows shorten it by finding new routes over the floodplain. Our model mechanics thus come into play during two phases of planform evolution in a freely meandering river channel: first during initial pattern formation, and again when overbank flow

forces new interaction with the floodplain. Between these two phases, migration dynamics will dominate channel planform behavior.

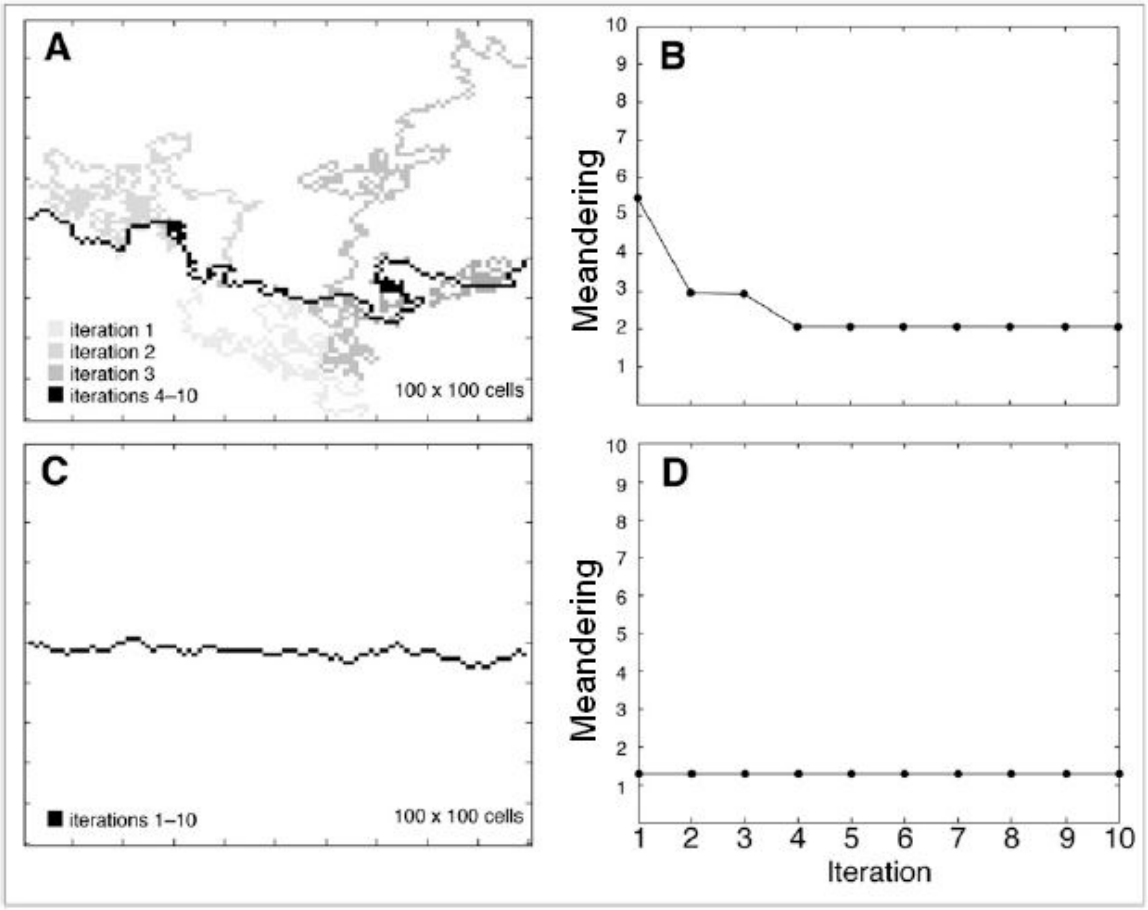

Figure. 3 Theoretically, Meandering has no upper bound. However, where channel migration occurs in natural systems, flow dynamics tend to not only create excursive meanders but also cut them off, episodically shortening the overall channel length and reducing Meandering. In the absence of a cutoff mechanism, resistance-dominated conditions (*R/S* >> 1) in this model will produce super Meander patterns that are more numerical artifacts than useful analogs, a problem others have also encountered. It is affected that a cutoff-like function by updating and iterating the domain to allow the flow path to find a minimum length for a given combination of *R* and *S* that excludes numerical artifacts of super Meander paths from the compiled results, particularly when *R* >> *S.(A)* Example of iterated flow paths and *(B)* corresponding meanderings for *R* = 0.04 and *S* = 0.001. *C* and *D* show the comparatively locked planform of a slope-dominated, low-Meandering channel (*R* = 0.001 and *S* = 0.04).

The number of floodplain Froude may extend to adjustments in channel Meandering connected to land-use changes that reflect roughness characteristics of the floodplain. The literature of land-use history in the Pachmarhis, India has linked deforestation in riparian corridors to morphological changes in fluvial channels (29). Similarly, historical maps and descriptions of the Sacramento River in California (30) indicate that before at least 1874, the river followed the Meander channel (Ω = 2.2) shown in Fig. 9, and was flanked by natural riparian vegetation. That vegetation was subsequently cleared and replanted in orchards; by 1898 multiple incidents of meander cutoff had straightened the channel to the path shown in white (22 = 1.4). Given the valley slope along this reach ($S = 3.3 \times 10^{-5}$) (31), the cutoff-driven change in Meandering may be explained as a function of a change in resistance *R* reflecting the transition from local riparian vegetation to orchard plantations (30, 31). In terms of our application of Manning's n, this would represent a decrease from $n = 0.10$-0.15 to $n = 0.05$(Fig. 8).

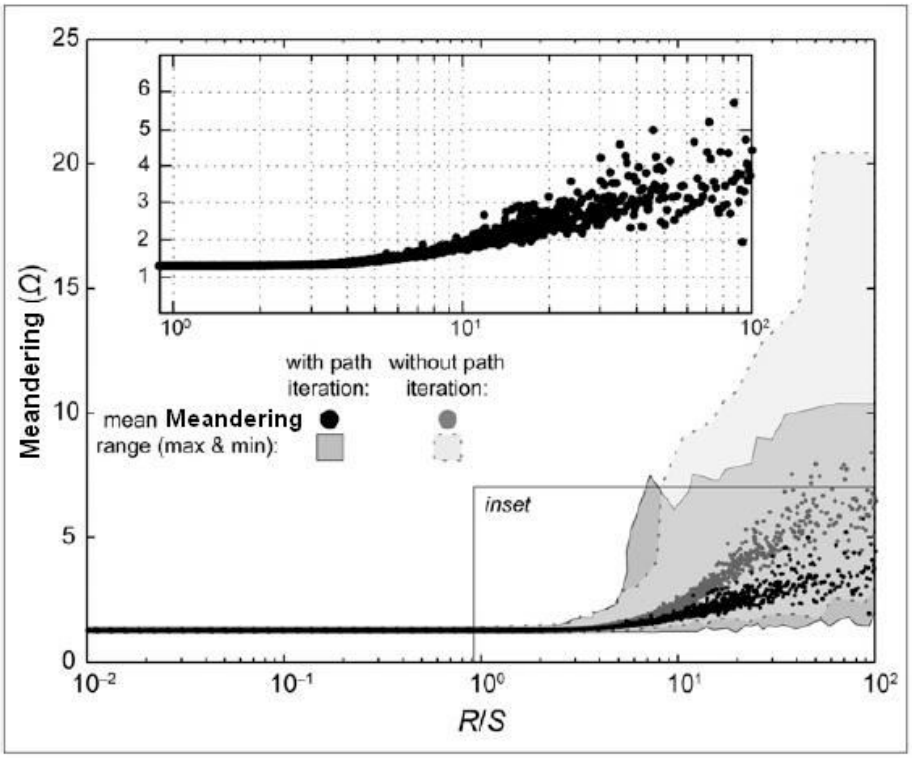

Figure. 4. Semilog plot showing ensemble results of modeled Meandering (Ω) versus relative resistance *(R/S)*. Shaded regions illustrate the range (maxima to minima) of meanderings produced by the model with (dark region) and without (light region) the iteration rule to shorten super Meander paths. Black dots and gray dots show the mean meanderings for both cases, respectively. *Inset* shows in greater detail mean meanderings generated with the iteration rule. Additional statistical properties of the model are provided in Fig.5

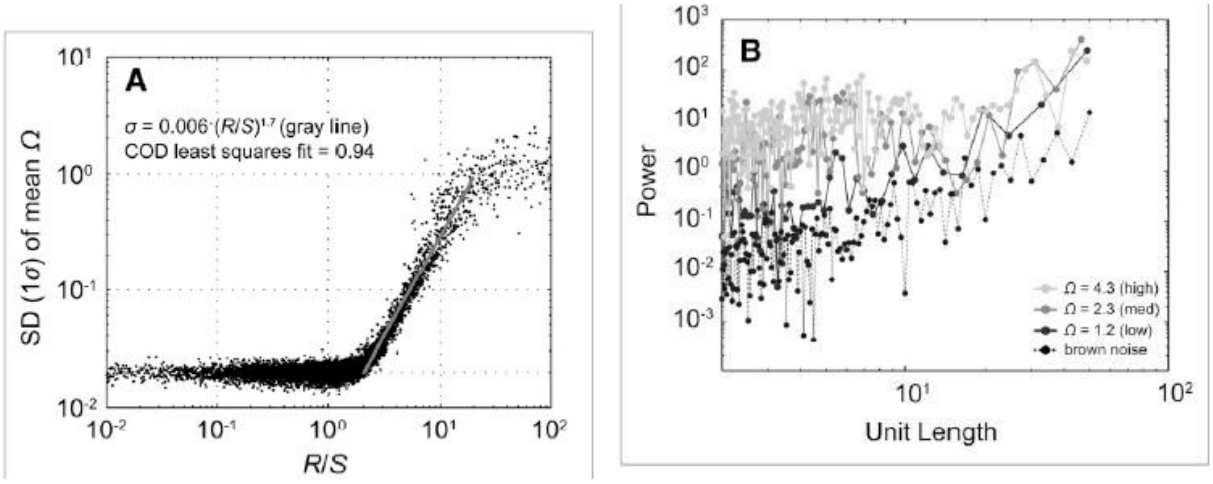

Figure. 5. (A) SD versus *R/S* of ensemble model runs. Variance scales with mean *R/S*.(B) Power spectra of representative modeled low-, medium-, and high-Meandering planforms, with the power spectrum for a brown-noise signal (integral of a white-noise signal) for comparison. The model does not produce planforms with a preferred wavelength. Both A and B are indicative of the model's fundamentally Brownian structure.

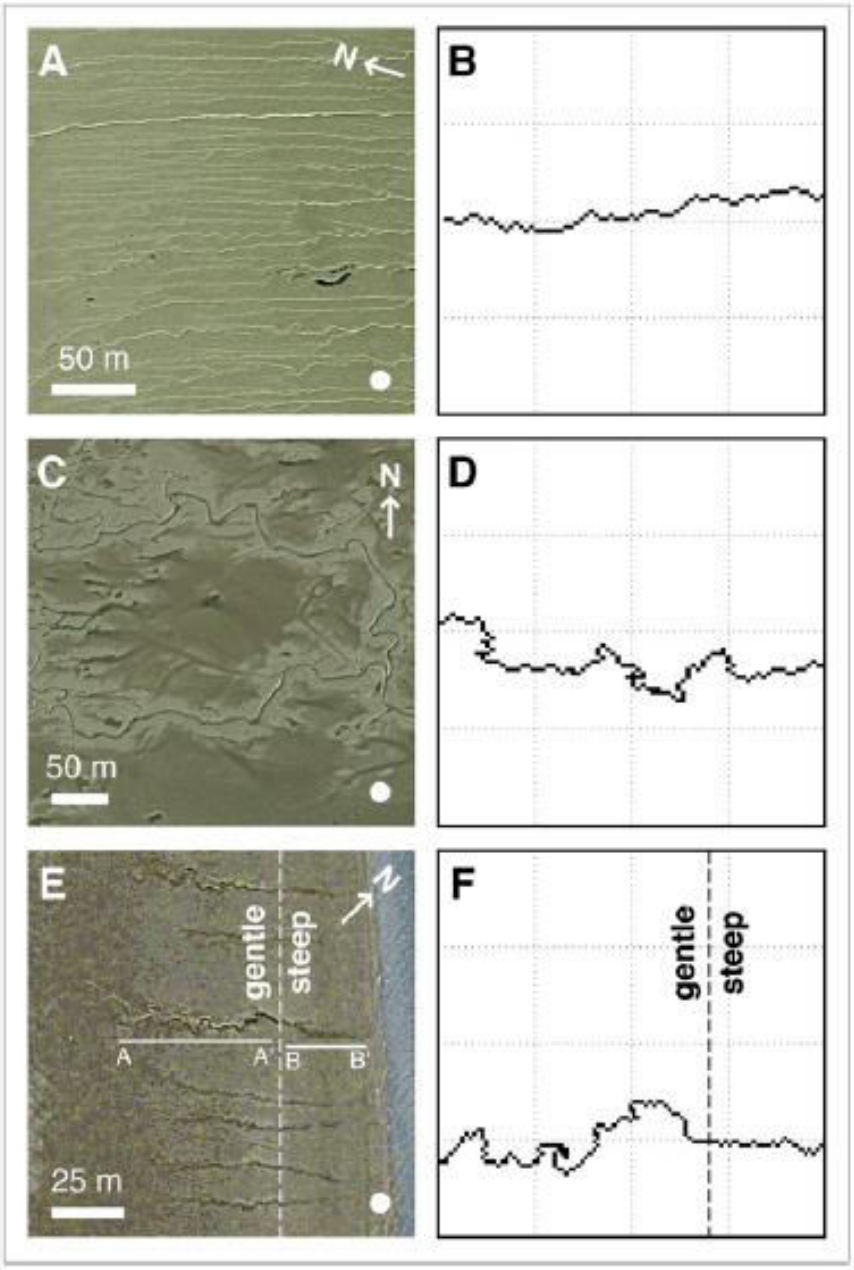

Figure. 6. Comparisons of channels in intertidal mudflats and simulated plan-forms. (*A*) Low-Meandering channels in an intertidal river bank and (*B*) a simulated low-Meandering channel *(R* = 0.005; *S* = 0.01; *R/S* = 0.5). (*C*)High-Meandering channels in an intertidal mudflat and (*D*) a simulated high-Meandering channel (*R* = 0.005; *S* = 0.001; *R/S* = 5). (*E*) Intertidal channels that cross a break in slope (dotted line) from gentle (*A-A'*) to steep (*B-B'*), and (*F*) a simulated channel over a slope break based on (*E*) (25), where *S* ~ 0.005 between *A and A'* and *S* ~ 0.04 between *B* and *B',* using a resistance of *R* ~ 0.05 derived from Fig. 2.

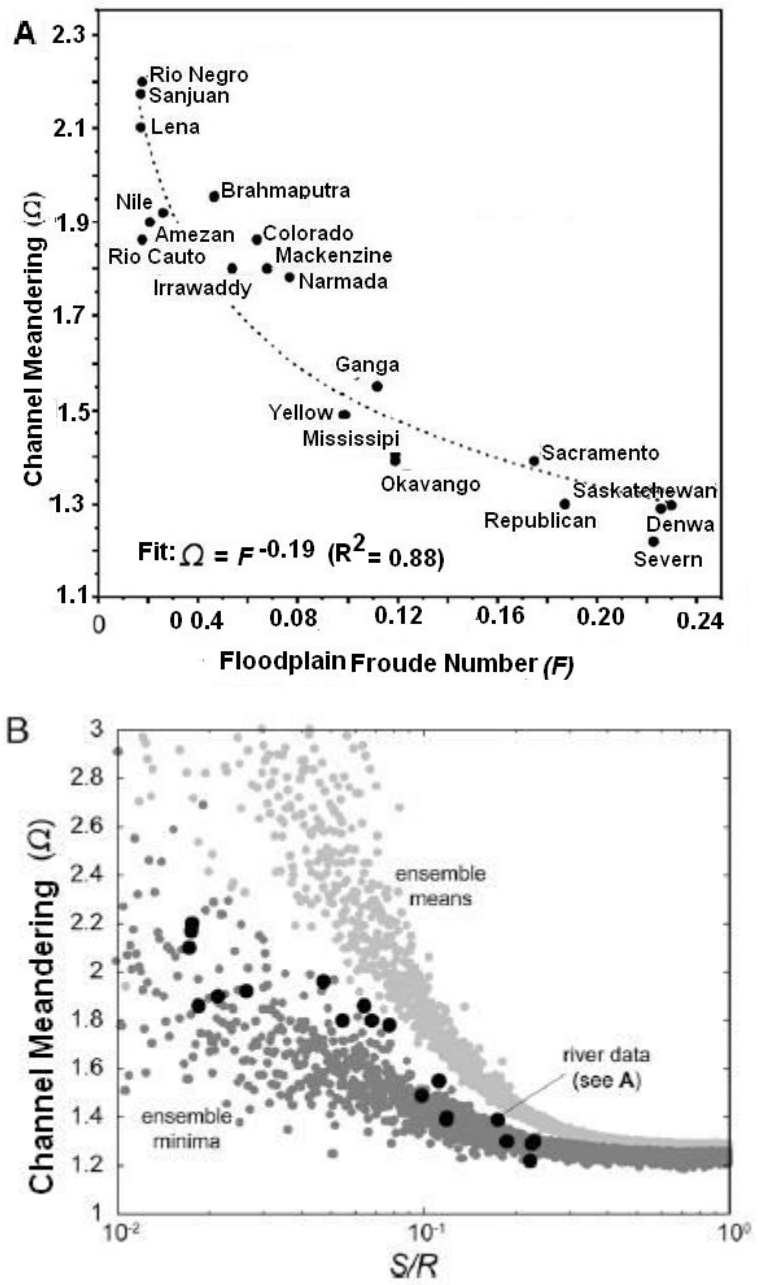

Figure. 7. (*A*) Meandering versus floodplain Froude number for 20 rivers around the world. Details regarding these data and their sources are available in (B) Semilog plot of ensemble means (light gray dots) and minima (dark gray dots) of modeled Meandering versus *S/R*, in keeping with the Froude number convention used in A and Eq. 6. Data from *A* are superimposed (large black dots).

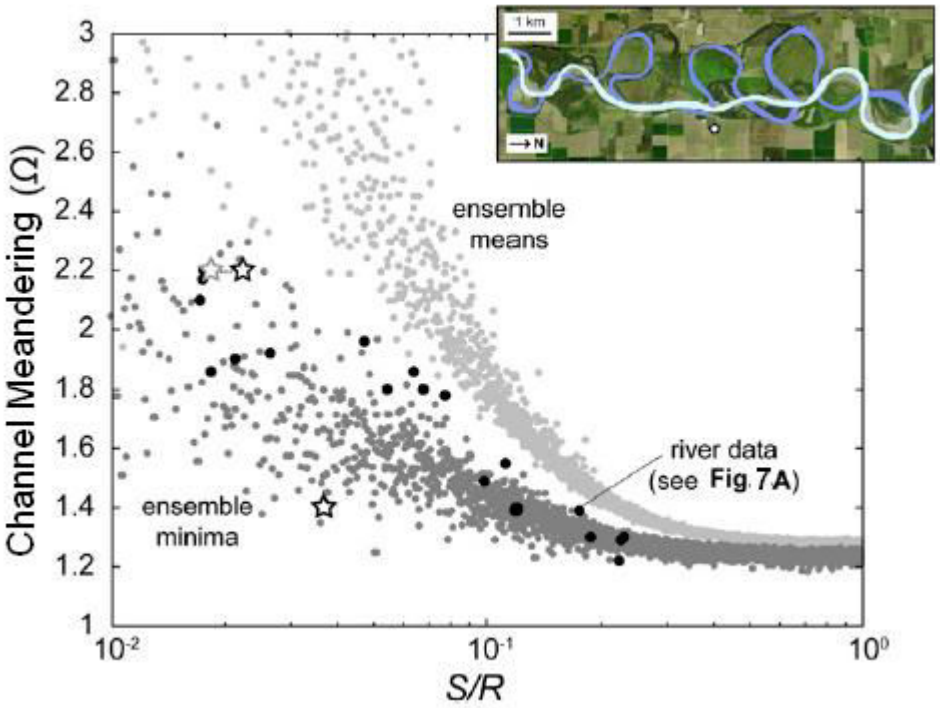

Figure. 8. Historical changes in the Sacramento River planform in terms of floodplain Froude number, plotted atop the data in Fig. 7 B. The linked gray and black star symbols at Ω= 2.2 mark the difference between assuming Manning's n = 0.15 (gray) or n = 0.10 (black) for the natural floodplain before 1874. Star symbol at Ω = 1.4 reflects the effect of orchard plantations (here, n = 0.05) after 1898.

Discussion

The resistance parameter R in this model is an extract of physical flow impediments but is not truly theoretical: for a given surface, R might be decided from a high-resolution digital field map, similar to light detection and ranging (LIDAR) survey or laser scan of a laboratory flume. Investigations of lunar and Venusian rilles have suggested that rille meandering likely depends on preexisting conditions of landscape topography and slope (12, 13). Consider, as a conceptual example, the lunar

Figure. 9. Land-use studies that alter riparian vegetation density, which changes floodplain resistance, which affect channel Meandering. It reflects that the Sacramento River (California), Meandering decreased from Ω = 2.2 before 1874 (blue) to Ω = 1.4 by 1898 (white) after natural vegetation was altered with planted orchards. The present and historical river conditions is related to data in Fig. 7 *B* and Fig. 8

landscape in Fig. 1*F*. A high-resolution topographic map would capture the subtle undulations in the surface underlying the rille. Subtracting mean slope of that surface from the elevation data leaves residuals that constitute the topographic variability; the maximum absolute value of those residuals is R,

the upper limit of the range of topographic resistance 0-*R*.Ifmudflats are of interest, then a sensitive resolution of micro topography would likely allow a comparable analysis. LIDAR surveys of vegetated environments typically separate laser "first return" from "last return" as a way of distinguishing between the canopy and the ground (or "bare earth"). Calculating *R* solely from last-return measurements of topographic variability would neglect vegetation's role in flow resistance, but measuring vegetation-density distributions in the first-return data as factors of floodplain resistance, beyond informing a Manning's *n* classification, could produce a more comprehensive approximation of *R*. In a long-duration laboratory flume experiment in which floodplain vegetation (such as alfalfa sprouts) and the channel planform coevolve, *R* would change over time as a function of vegetation growth, which repeated topographic laser scans of the flume apparatus could record.

Like Manning's *n*, the friction factor in the Darcy-Weisbach equation for head loss, or a drag force on woody riparian vegetation (11, 32), the resistance term *R* in this model is a flow-resistance term. It is reiterated that *R*, is appropriated and does not represent substrate erodibility. Substrate erodibility and bank stability, which can be functions of material properties and vegetation root systems, are certainly essential to the mechanisms that drive channelization and channel-migration behaviors. Positive correlation between erodibility and channel Meandering suggests rock weakness is a primary control on Meandering in bedrock rivers (7, 10). Recent laboratory attempts to isolate the conditions sufficient for sustaining a meandering, Meander channel have highlighted the importance of increased bank strength relative to bed material, where bank strength is a function of sediment cohesiveness, stabilization by vegetation, or a combined effect (5, 6, 21). A channel-planform model based on flow resistance does not replace these elements, but can nevertheless inform investigations of planform origins even in systems where erodibility is important. Collectively, the meanderings in our model derived from random walks constrained only by resistance and slope comprise a set of simplest-case explanations, a template of null hypotheses that help isolate and clarify more complicated, specific, or dynamic factors driving planform evolution.

Even though the theoretical template does not explicitly forcast the multichannel planforms (e.g., anastomosing, braided) that available in nature, individual channel threads within such planforms—where individual threads can be differentiated—should share a similar dependence on local resistance and slope. Conventionally, Meandering is a metric exclusive to single-thread channels. For example, it is unclear what would constitute a single-thread reach of a braided channel during normal flow conditions. A simple anastomosing pattern is perhaps a more manageable thought experiment: where flow divides among several intertwined routes, Meandering for each determined "thread" could be calculated separately; together, those meanderings would represent the Meandering range the floodplain will support, as the model is used to suggest.

The genuine application of relative resistance (*R/S*) may be to intimate how floodplains of artificially straightened rivers are examined for restarting riparian ecosystems (33). Stream flow at the local scale of a channel Meandering at the larger scale of the river planform are important to a river's physical and ecological dynamics: even as internal flows amend the channel at a given bend, the overall planform sets the conditions for in-stream flow (9) and, by extension, in-stream habitats. Channel Meandering will still reflect the characteristic resistance of the flood-plain even in fluvial systems dominated by migration dynamics (e.g., Fig. 7). If a channel needs a large R/S to be highly Meander, then even a channel engineered to be Meander will tend to straighten if the R/S ratio of its floodplain is suppressed or inherently low and if overbank flows are allowed to mobilize the floodplain surface. Alternatively, increasing appropriate flood-plain resistance might foster a channel more Meander than extant hydraulic geometry may predict. Narrow rivers in densely forested regions, for example, appear to owe their channel patterns to log jams and other woody debris obstructions (29); log jams are thus an obstructive type of floodplain resistance that deforestation removes but reforesting can restore.

Conclusions

It is demonstrated how two intrinsic properties of a landscape surface—slope (*S*) and resistance (*R*)—can exert a first-order control on flow-path Meandering. Paradoxical findings of static and dynamic

flow patterns motivate the analysis: explanations for Meandering that hinge on migration dynamics do not decipher easily to static Meander planforms; likewise, as others have noted (21), vegetation-driven explanations for planform Meandering cannot extend to the same patterns in unvegetated environments. Although erodibility exerts a principal control on channelization and flow dynamics within a channel, flow resistance is arguably a more general condition applicable to a greater variety of single-thread flows. The resistance parameter *R* informs the range of possible meanderings a given landscape might support. Independent of internal flow forces, *R* is potentially useful in remote remote-sensing applications and anywhere in-channel data are lacking or unobtainable. For example, determination of *R* might inform requisite conditions for sustainable Meandering in engineered streams. The relationships that propose is an explication of Meandering enough to account for the ubiquity of Meander channel patterns in nature and not conflict with the various mechanistic processes from which specific channel types can derive.

Acknowledgments.

I would like to thank Mr. Nripendra Dongre who contributed excellent reviews that greately improved the IT work. I also express my sincere thanks to Mr. Ashokan CH and Mr. Pankaj Tripathi for supporting the research works in person.

References

1. Schumm SA, Khan HR (1972) Experimental study of channel patterns. *Geol Soc Am Bull* 83(6):1755.
2. Hooke JM (2007) Complexity, self-organisation and variation in behaviour in meandering rivers. *Geomorphology* 91(3-4):236-258.
3. Howard AD, Knutson TR (1984) Sufficient conditions for river meandering - A simulation approach. *Water Resour Res* 20(11):1659-1667.
4. Stolum HH (1996) River meandering as a self-organization process. *Science* 271(5256):
5. 1710-1713.
6. Tal M, Paola C (2007) Dynamic single-thread channels maintained by the interaction of flow and vegetation. *Geology* 35(4):347-350.
7. Braudrick CA, Dietrich WE, Leverich GT, Sklar LS (2009) Experimental evidence for the conditions necessary to sustain meandering in coarse-bedded rivers. *Proc Natl AcadSci USA* 106(40):16936-16941.
8. Stark CP, et al. (2010) The climatic signature of incised river meanders. *Science*327(5972):1497-1501.
9. Ikeda S, Parker G (1989) *River Meandering,* (American Geophysical Union, Washington,DC), Vol 12.
10. Furbish DJ (1991) Spatial autoregressive structure in meander evolution. *Geol Soc Am Bull* 103(12):1576-1589.
11. Harden DR (1990) Controlling factors in the distribution and development of incised meanders in the Central Colorado Plateau. *Geol Soc Am Bull* 102(2):233-242.
12. Finnegan NJ, Dietrich WE (2011) Episodic bedrock strath terrace formation due to meander migration and cutoff. *Geology* 39(2):143-146.
13. Greeley R (1971) Lunar Hadley Rille: Considerations of its origin. *Science* 172(3984): 722-725.
14. Komatsu G, Baker VR (1994) Meander properties of Venusian channels. *Geology* 22(1):67-70.
15. Allen JRL (2000) Morphodynamics of Holocene salt marshes: A review sketch from the Atlantic and Southern North Sea coasts of Europe. *Quat Sci Rev* 19(12):1155-1231.
16. D'Alpaos A, Lanzoni S, Marani M, Fagherazzi S, Rinaldo A (2005) Tidal network ontogeny: Channel initiation and early development. *J Geophys Res* 110(F2):1 -14.
17. Goldthwaite JW (1937) Unchanging meanders of tidal creeks. *Proc Geol Soc Am* 1:73-74.
18. Leopold LB, Langbein WB (1962) The *concept of entropy in landscape evolution.US* Geological Survey Professional Paper, Vol 500A.
19. Surkan AJ, Vankan J (1969) Constrained random walk meander generation. *WaterResour Res* 5(6):1343.
20. Hammersley JM, Welsh DJA (1980) Percolation theory and its ramifications. *ContempPhys* 21(6):593-605.
21. Jogi P, Sornette D (1998) Self-organized criticalrandom directed polymers. *PhysRevE*57(6):6936-6943.
22. Howard AD (2009)Howtomakea meandering river. *ProcNatlAcadSciUSA*106(41): 17245-17246.
23. Lancaster ST, Bras RL (2002) A simple model of river meandering and its comparison to natural channels. *Hydrol Processes* 16(1):1 -26.
24. Seminara G (2006) Meanders. *J FluidMech* 554:271-297.Perron JT, Fagherazzi S (2012) The legacy of initial conditions in landscape evolution. *Earth Surf Processes Landforms* 37(1):52-63.

25. KleinhansMG,Schuurman F,BakxW,MarkiesH (2009)Meanderingchanneldynamics in highly cohesive sediment on an intertidal mud flat in the Westerschelde estuary, the Netherlands. *Geomorphology*105(3-4):261-276.
26. Chow VT (1959) *Open Channel Hydraulics* (McGraw-Hill, New York).
27. SpeightJG (1965)Meander spectra oftheAngabunga River, Papua. *J Hydrol(AmsterdamNeth)* 3:1 -15.
28. Stolum HH (1998) Planform geometry and dynamics of meandering rivers. *Geol SocAm Bull* 110(11):1485-1498.
29. CollinsBD,MontgomeryDR,HaasAD (2002)Historicalchangesin thedistribution and functions of large wood in Puget Lowland rivers. *Can J Fish Aquat Sci* 59(1):66-76.
30. Sullivan DG (1982) Prehistoric flooding in the Sacramento Valley: Stratigraphic evi-dencefrom LittlePackerLake,Glenn County,California. MSthesis(UnivofCalifornia, Berkeley, CA).
31. ConstantineJA,McLean SR,DunneT (2010)Amechanism ofchutecutoffalong large meandering rivers with uniform floodplain topography. *Geol Soc Am Bull* 122(5-6):855-869.
32. Smith JD (2004) The role of riparian shrubs in preventing floodplain unraveling along the Clark fork of the Columbia River in the Deer Lodge Valley, Montana. *Riparian Vegetation and Fluvial Geomorphology,* eds Bennett SJ, Simon A, Vol 8, pp 71 -85.
33. Beechie TJ, et al. (2010) Process-based principles for restoring river cosystems. *Bioscience* 60(3):209-2